Title

Metabolomics reveals mycoplasma contamination interferes with the metabolism of PANC-1 cells

Journal

Analytical and Bioanalytical Chemistry, 408(16)

ISSN

1618-2642

Authors

Yu, Tao
Wang, Yongtao
Zhang, Huizhen
et al.

Publication Date

2016-06-01

DOI

10.1007/s00216-016-9525-9

Peer reviewed

HHS Public Access

Author manuscript

Anal Bioanal Chem. Author manuscript; available in PMC 2018 December 20.

Published in final edited form as:

Anal Bioanal Chem. 2016 June ; 408(16): 4267–4273. doi:10.1007/s00216-016-9525-9.

Metabolomics reveals mycoplasma contamination interferes with the metabolism of PANC-1 cells

Tao Yu[#1], **Yongtao Wang**[#1], **Huizhen Zhang**[1], **Caroline H. Johnson**[2], **Yiming Jiang**[1], **Xiangjun Li**[3], **Zeming Wu**[3], **Tian Liu**[3], **Kristopher W. Krausz**[4], **Aiming Yu**[5], **Frank J. Gonzalez**[4], **Min Huang**[1], and **Huichang Bi**[1]

[1] School of Pharmaceutical Sciences, Sun Yat-sen University, 132# Waihuandong Rd, University City of Guangzhou, Guangzhou 510006, China

[2] Department of Environmental Health Sciences, Yale School of Public Health, Yale University, 60 College Street, New Haven, CT 06520, USA

[3] Thermo Fisher Scientific, Xin Jinqiao Rd., Shanghai 201206, China

[4] Laboratory of Metabolism, Center for Cancer Research, National Cancer Institute, NIH, Bethesda, MD 20892, USA

[5] Department of Biochemistry and Molecular Medicine, UC Davis Medical Center, Sacramento, CA 95817, USA

[#] These authors contributed equally to this work.

Abstract

Mycoplasma contamination is a common problem in cell culture and can alter cellular functions. Since cell metabolism is either directly or indirectly involved in every aspect of cell function, it is important to detect changes to the cellular metabolome after mycoplasma infection. In this study, liquid chromatography mass spectrometry (LC/MS)-based metabolomics was used to investigate the effect of mycoplasma contamination on the cellular metabolism of human pancreatic carcinoma cells (PANC-1). Multivariate analysis demonstrated that mycoplasma contamination induced significant metabolic changes in PANC-1 cells. Twenty-three metabolites were identified and found to be involved in arginine and purine metabolism and energy supply. This study demonstrates that mycoplasma contamination significantly alters cellular metabolite levels, confirming the compelling need for routine checking of cell cultures for mycoplasma contamination, particularly when used for metabolomics studies.

Keywords

Mycoplasma contamination; Metabolomics; Cellular metabolism; PANC-1 cells; Cell culture

Compliance with ethical standards

Conflict of interest The authors declare that they have no conflicts of interest.

Introduction

Mycoplasma, the smallest and simplest self-replicating bacteria, are widely distributed in nature [1, 2]. They have limited biosynthetic ability and grow in close relationship with mammalian cells as parasites [3–5]. Infection with mycoplasma is a frequently observed problem in cell cultures. It is estimated that up to 35 % and even 80 % of cell cultures in current use are infected with various mycoplasma species [6]. Contamination of cell cultures with mycoplasma presents a challenging issue in terms of detectability and prevention since no overt changes are observed in media pH, turbidity, and direct microscopic visualization [3, 4, 7]. In general, mycoplasma adheres to the host cell surface and some species may even invade the host cell for biosynthesis of macromolecules [8, 9]. Many influences of mycoplasma on cell culture parameters have been described. The consequences of an infection for the host cells are variable, ranging from no apparent effect to induction of severe biological events. It has been reported that mycoplasma-contaminated cells can have up to 15-fold resistance to doxorubicin, vincristine, and etoposide in tetrazolium-based MTT assay [10]. Mycoplasma presence due to cell culture contamination is able to efficiently and rapidly degrade extracellular amyloid-beta peptide. *Mycoplasma fermentans* also stimulated prostaglandin E2 production, and *Mycoplasma hyorhinis* infection exerted a significant impact on L-arginine metabolism [11–13]. Additionally, dendritic cells can sense mycoplasma infection and mature as they do in response to most viruses and bacteria, indicating that mycoplasma contamination could induce dendritic cell maturation [14, 15]. These findings suggest mycoplasma can change cell metabolism and then alter various cell functions. Since cell metabolism is either directly or indirectly involved in every aspect of cell function, it is important to detect the changes to the cellular metabolome after mycoplasma infection.

Metabolomics analysis of cells has emerged as an important approach for studying cellular biochemistry, revealing information reflecting changes to the metabolome, metabolic pathways, and biochemical reactions occurring within the cells [16].

In this study, the human pancreatic cancer cell line PANC-1 was used as a cell culture model to study changes to the cellular metabolome after mycoplasma infection. Liquid chromatography mass spectrometry (LC/MS)-based metabolomics was used to analyze the metabolome of mycoplasma contaminated PANC-1 cells and mycoplasma-free PANC-1 cells. It was found that mycoplasma contamination induced significant metabolic perturbations in PANC-1 cell line. Metabolites that were abundant at different levels and statistically significant were tentatively identified. Functions of these metabolites and their involvement in metabolic pathways were summarized. Our findings provide direct evidence for a mycoplasma-induced cellular metabolome shift and confirm the compelling need for routine checking of cell cultures for mycoplasma contamination, particularly in cellular metabolomics studies.

Materials and methods

Cell culture

Uncontaminated human pancreatic carcinoma PANC-1 cells were purchased from American Type Culture Collection (Manassas, VA). PANC-1 cells were cultured in mycoplasma-free DMEM containing 10 % FBS, 100 IU/mL penicillin sodium, and 100 μg/mL streptomycin sulfate at 37 °C in a 5 % CO_2 atmosphere. All other chemicals and solvents were commercially available and of analytical grade.

Mycoplasma detection and anti-mycoplasma treatment

During routine culture maintenance, a subculture of PANC-1 cells was inadvertently contaminated with mycoplasma. PANC-1 cells were checked for mycoplasma infection using Hoechst 33258 DNA staining (Beyotime, Jiangsu, China) according to the manufacturer's instructions. Mycoplasma-infected PANC-1 cells were treated with Plasmocin 25 μg/ mL for 14 consecutive days. Culture medium was removed and replaced with fresh Plasmocin-containing medium every 3–4 days according to the manufacturer's instructions. After a 14-day treatment, cells were confirmed to be mycoplasma negative, used as mycoplasma-free samples, and further cultured in DMEM media in the absence of Plasmocin. For positive control, mycoplasma-infected PANC-1 cells were cultured for 14 consecutive days in DMEM media in the absence of Plasmocin.

Cell samples

For sample collection, the cells were subcultured in 100-mm polystyrene Petri dishes at a density of 5×10^4 cells/dish and were grown to reach approximately 90 % confluence. Subsequently, the cells were quenched with liquid nitrogen and harvested by scraping as previously described [17]. Then 900 μL chilled (−20 °C) MeOH was added to 300 μL cell suspension. The mixture was vigorously vortexed and then centrifuged at 14,000×*g* for 15 min at 4 °C to precipitate proteins and particulates. One milliliter of supernatant was transferred to a clean tube and dried under nitrogen flow at room temperature. The residuals were resuspended using 200 μL 70 % ACN/water and then centrifuged at 14,000×*g* at 4 °C for 5 min. Finally, an aliquot (5 μL) of the supernatant was injected for ultra-high performance liquid chromatography electrospray ionization mass spectrometry (UHPLC–ESI–MS) analysis.

Liquid chromatography–high-resolution mass spectrometry analysis

Hydrophilic interaction liquid chromatography (HILIC) separation was carried out by using an Atlantis Silica HILIC column (3 μm, 2.1 mm i.d. × 100 mm, Waters, Milford, MA, USA) on a Thermo Scientific Dionex Ultimate 3000 UHPLC system. Flow rate was 300 μL/min with column temperature at 40 °C. Binary mobile phases were (A) 5 % water in acetonitrile with 10 mM ammonium formate and 0.1 % formic acid and (B) 50 % water in acetonitrile with 10 mM ammonium formate and 0.1 % formic acid. Linear gradient was implemented as follows: 0–1.0 min holding at 100 % A, linearly increasing to 100 % B at 20 min, then washing column for the next 4.9 min, and equilibrating until 30 min. MS was operated with a Thermo Scientific Q Exactive™ benchtop Orbitrap mass spectrometer equipped with

heated ESI source in ESI positive and negative modes (Thermo Scientific, San Jose, CA). The samples were independently examined in both ESI positive and negative modes. Untargeted profiling analyses acquired the data at full scan mode (80–900 *m/z*) and 70,000 FWHM resolution followed by top-10 data-dependent MS/MS at 17,500 FWHM resolution. The main parameters for MS/MS included AGC target $1e^5$; maximum IT 70 ms; isolation window 2.0 *m/z*; normalized collision energy 15, 30, and 45 eV; apex trigger 5~10 s; and dynamic exclusion 10 s. Ionization conditions were optimized and finally operated at spray voltage 3.5/2.8 kV (+/–) and heater and capillary temperatures 350 and 325 °C, respectively. Total ion chromatograms and mass spectra from LC-HRMS runs were generated as raw files in Xcalibur (Thermo Scientific, San Jose, CA).

Data processing, analysis, and identification of metabolites

For untargeted profiling analysis, an optimized workflow was carried out for comprehensive metabolite phenotyping of the two cell groups and discovering differential metabolites. It consisted of background noise subtraction, automated peak detection and integration, peak alignment, multivariate principal component analysis (PCA), and univariate analysis, which was performed using Thermo Scientific label-free differential analysis bioinformatics software SIEVE 2.2 (Thermo Scientific, San Jose, CA) and SIMCA-P 13.0 (Umetrics, Kinnelon, NJ). Volcano plots were used to filter metabolites of interest that displayed both significant fold changes (fold change >2 or <−2) and statistical significance ($P<0.05$) between the two groups. Subsequently, these metabolites were putatively identified based on accurate mass match (accurate mass error ±5 ppm) and fragmentation pattern match. Putative structural annotation was carried out by searching the metabolite databases HMDB (http://www.hmdb.ca/), KEGG (http://www.genome.jp/kegg/), and METLIN (http://metlin.scripps.Edu.) using the mass-to-charge ratio of the metabolic features. Mz Cloud (https://www.mzcloud.org/) and METLIN were used for MS/MS spectral matching. TraceFinder™ software from Thermo Scientific was employed for routine quantitation in targeted metabolite analysis. A heatmap plot was also constructed from metabolites using MultiExperiment Viewer (http://www.tm4.org/mev). Finally, the functions of these metabolites and metabolic pathways were studied using the KEGG database (http://www.genome.jp/kegg/).

Results

In order to measure the effect of mycoplasma contamination on cell metabolism, cellular metabolomics analysis was performed. The comparison of total ion chromatograms (TIC) from representative samples from each of the two groups can be seen on the mirror plots in Fig. 1. Multiple notable differences were observed in peak intensities at the same retention time between the two TIC profiles, indicating a clear disparity in the metabolic profiles of mycoplasma-infected or uninfected cells.

To compare the overall variation within and between the metabolic profiles from the two groups, principal component analysis (PCA) was performed. Our results showed clear separation of mycoplasma-infected cells and mycoplasma-removed cells (Fig. 2), indicating that mycoplasma infection caused significant metabolic changes in the host cells. The

proximity of the replicate samples ($n = 5$) in the PCA scatterplots reflects the sample-to-sample variation. The PCA scatterplots showed that the samples representing metabolites of mycoplasma-infected cells had a bigger sample-to-sample variation.

Furthermore, the volcano plots revealed a number of metabolite features that were significantly changed (Fig. 3). Metabolite features of interest were selected by a fold change threshold of >2 as well as a P value <0.05 (depicted as green dots). Metabolites that were found to be abundant at similar levels or statistically nonsignificant between the two groups were excluded (depicted as red dots). Those selected metabolite features were further identified by comparison of retention times and MS/MS fragmentation patterns with authentic standards, or from the MS/MS fragmentation pattern annotated in the HMDB and METLIN databases. The detailed results are summarized in Table 1 to show the identified metabolites, the disturbed metabolic profiles, and metabolic pathways.

To further evaluate the changes to the cellular metabolome caused by mycoplasma infection, the relative response of the identified metabolites was compared. The heatmap in Fig. 4 shows the relative increase (red) or decrease (green) of each metabolite. Specifically, L-arginine and saccharopine were found to be significantly decreased in mycoplasma-infected cells under both positive and negative ESI modes while there was a significant increase in inosine, guanosine, adenine, and citrulline, which was observed in mycoplasma-infected cells.

Discussion

In this study, LC/MS-based metabolomics was used to compare the metabolism of PANC-1 cells after infection with mycoplasma. Our results revealed that the cellular metabolome was significantly influenced by mycoplasma contaminations.

Arginine metabolism

Arginine was remarkably decreased in mycoplasma-infected PANC-1 cells compared to that in uninfected cells, suggesting an interference in arginine metabolism. As an essential amino acid in cell cultures, arginine has profound effects on cell functions. Reduction of arginine further results in an abnormality of protein synthesis, cell division, and growth. Moreover, chromosomal damage can be caused due to the lack of arginine, which is required for histone synthesis in the nucleus [6, 18]. The impact of mycoplasma infection on L-arginine metabolism has been previously reported [13, 19]. Mycoplasma are able to use arginine as their major source of energy via the arginine dihydrolase pathway, while generating citrulline and ornithine [20, 21]. In agreement with these previous findings, a depletion of L-arginine and elevated citrulline and ornithine production were observed in cell samples infected by mycoplasma.

Purine metabolism

For mycoplasma-contaminated PANC-1 cells, purine bases adenine and guanine as well as the nucleosides inosine and guanosine were elevated compared to mycoplasma-free cell samples. Inosine 5′-monophosphate (IMP) was also increased in mycoplasma-contaminated

samples. The changes to these metabolites indicate an interference in purine metabolism after mycoplasma contamination.

In mammalian cells, purine nucleotides can be synthesized in two distinct pathways, including de novo synthesis and salvage of either exogenous or endogenous purines. Mycoplasma are unable to synthesize purine bases de novo, but are capable of importing precursors from the environment via salvage pathways [22, 23]. The associated enzymes are adenine phosphoribosyltransferase (APRT) and hypoxanthine-guanine phosphoribosyltransferase (HGPRT), which convert adenine, hypoxanthine, as well as guanine, into adenine 5′ monophosphate (AMP), inosine 5′ monophosphate (IMP), and guanine 5′ monophosphate (GMP), respectively [24]. In this study, the elevated levels of IMP in mycoplasma-contaminated cells were probably due to the enhanced purine salvage pathways.

Another enzyme associated with the nucleotide salvage pathway is purine nucleoside phosphorylase (PNP). PNP metabolizes adenosine into adenine, guanosine into guanine, and inosine into hypoxanthine, in each case producing ribose-1-phosphate. Adenosine phosphorylase has never been detected in mammalian cells but, like other PNPs, is commonly present in many mycoplasma species [25]. The accumulation of adenine and guanine could be due to the reversible conversion of corresponding nucleotides by PNPs. It was reported that in specific mycoplasma species, e.g., *Mycoplasma lipophilium*, adenosine is converted into inosine by deamination [25]. Therefore, here, the increased level of inosine could be caused by contamination of this specific mycoplasma. In addition, specific mycoplasma extract has been reported to catalyze reactions of degradating GMP to guanosine [26], which might explain the elevated level of guanosine in mycoplasma-contaminated PANC-1 cells.

A decreased level of D-serine was also observed in mycoplasma-contaminated cells compared to mycoplasma-free samples. Serine is synthesized from 3-phosphoglycerate and is the precursor to several biomolecules, including glycine and cysteine [27]. It also participates in the biosynthesis of purines and pyrimidines. Its reduction signifies interference in its anabolism.

Energy supply

Elevated levels of gluconic acid and sedoheptulose 7-phosphate were observed in the mycoplasma-contaminated PANC-1 cells. Both metabolites are intermediates of the pentose phosphate pathway which result in generating NADPH used in intracellular reductive syntheses reactions and producing ribose 5-phosphate used in the synthesis of nucleic acids [28]. The increased levels of these metabolites signifies interference with these associated pathways.

Phosphoenol pyruvate and aconitic acid were also increased in mycoplasma-contaminated samples. In normal pyruvate metabolism, phosphoenol pyruvate is converted to pyruvate, which enters the tricarboxylic acid (TCA) cycle for adenosine triphosphate (ATP) production [29, 30]. Produced by the dehydration of citric acid, aconitic acid is also an intermediate in the TCA cycle [31]. Hence, accumulation of these two metabolites could

demonstrate interference of the TCA cycle and interference with key energy metabolism intermediates in mycoplasma-contaminated cells.

Other metabolic pathways affected by mycoplasma contamination

Saccharopine, an intermediate in the degradation of lysine [32, 33], was significantly decreased in mycoplasma infected PANC-1 cells in both positive and negative modes. It was reported that mycoplasma was able to assimilate lysine as a source of energy supply [34]. Although lysine was not identified, the reduction of saccharopine might be due to the assimilation of lysine by mycoplasma.

Mycoplasma-contaminated PANC-1 cells also exhibited a decreased level of CDP-choline compared to mycoplasma-free samples. Choline is an essential component which provides structural integrity and affects the signaling functions of the cell membranes, as well as lipid transport and metabolism [35]. Choline depletion of cell culture was induced by mycoplasma infection and was associated with the apoptotic death of the cells [36]. CDP-choline is an essential intermediate in the biosynthetic pathway of structural phospholipids in cell membranes. The decreased level of CDP-choline manifests inference with its metabolism.

In summary, our findings provide direct evidence that the cellular metabolome can be significantly affected by mycoplasma infection in PANC-1 cells; arginine metabolism, purine metabolism, amino acid biosynthesis, the TCA cycle, and energy supply were significantly affected by mycoplasma. These data show that mycoplasma contamination significantly alters cellular metabolite levels. On the basis of these results, we recommend the assessment of mycoplasma contamination prior to cell-based studies, particularly for studies involving cellular metabolism.

Acknowledgments

This work was financially supported by the Natural Science Foundation of China (Grants 81522047, 81573489, 81373470, 81320108027), the Natural Science Foundation of Guangdong Province (Grant 2015A030313124), and the Guangzhou Health Care Collaborative Innovation Program (Grant 201508020250).

References

1. Mycoplasmatales. RSaFE Bergey’s manual of systematic bacteriology. New York: Williams and Wilkins; 1984.
2. Razin S The genera mycoplasma U, achole- plasma, anaeroplasma, and astero-leplasma The prokaryotes. 2nd ed. New York: Springer; 1991.
3. Nikfarjam L, Farzaneh P. Prevention and detection of mycoplasma contamination in cell culture. Cell J. 2012;13(4):203–12. [PubMed: 23508237]
4. Rottem S, Barile MF. Beware of mycoplasmas. Trends Biotechnol. 1993;11(4):143–51. [PubMed: 7763647]
5. Hay RJ, Macy ML, Chen TR. Mycoplasma infection of cultured cells. Nature. 1989;339(6224):487–8. [PubMed: 2725683]
6. Drexler HG, Uphoff CC. Mycoplasma contamination of cell cultures: incidence, sources, effects, detection, elimination, prevention. Cytotechnology. 2002;39(2):75–90. [PubMed: 19003295]
7. Young L, Sung J, Stacey G, Masters JR. Detection of mycoplasma in cell cultures. Nat Protoc. 2010;5(5):929–34. [PubMed: 20431538]

8. Rottem S Interaction of mycoplasmas with host cells. Physiol Rev. 2003;83(2):417–32. [PubMed: 12663864]

9. Ueno PM, Timenetsky J, Centonze VE, Wewer JJ, Cagle M, Stein MA, et al. Interaction of mycoplasma genitalium with host cells: evidence for nuclear localization. Microbiology. 2008;154:3033–41. [PubMed: 18832309]

10. Denecke J, Becker K, Jurgens H, Gross R, Wolff JEA. Falsification of tetrazolium dye (MTT) based cytotoxicity assay results due to mycoplasma contamination of cell cultures. Anticancer Res. 1999;19(2A):1245–8. [PubMed: 10368683]

11. Zhao H, Dreses-Werringloer U, Davies P, Marambaud P. Amyloid-beta peptide degradation in cell cultures by mycoplasma contaminants. BMC Res Notes. 2008;1:38. [PubMed: 18710491]

12. Elkind E, Vaisid T, Kornspan JD, Barnoy S, Rottem S, Kosower NS. Neuroprotective effects of Mycoplasma hyorhinis against amyloid-beta-peptide toxicity in SH-SY5Y human neuroblastoma cells are mediated by calpastatin upregulation in the mycoplasma-infected cells. Neurochem Int. 2011;58(4):497–503. [PubMed: 21219955]

13. Krausse-Opatz B, Schmidt C, Fendrich U, Bialowons A, Kaever V, Zeidler H, et al. Production of prostaglandin E-2 in monocytes stimulated in vitro by Chlamydia trachomatis, Chlamydophila pneumoniae, and Mycoplasma fermentans. Microb Pathog. 2004;37(3):155–61. [PubMed: 15351039]

14. Salio M, Cerundolo V, Lanzavecchia A. Dendritic cell maturation is induced by mycoplasma infection but not by necrotic cells. Eur J Immunol. 2000;30(2):705–8. [PubMed: 10671230]

15. Chen XC, Chang LJ. Mycoplasma-mediated alterations of in vitro generation and functions of human dendritic cells. J Biomed Sci. 2005;12(1):31–46. [PubMed: 15864737]

16. Birungi G, Chen SM, Loy BP, Ng ML, Li SFY. Metabolomics approach for investigation of effects of dengue virus infection using the EA hy926 cell line. J Proteome Res. 2010;9(12):6523–34. [PubMed: 20954703]

17. Bi H, Krausz KW, Manna SK, Li F, Johnson CH, Gonzalez FJ. Optimization of harvesting, extraction, and analytical protocols for UPLC-ESI-MS-based metabolomic analysis of adherent mammalian cancer cells. Anal Bioanal Chem. 2013;405(15):5279–89. [PubMed: 23604415]

18. Paton GR, Jacobs JP, Perkins FT. Chromosome changes in human diploid-cell cultures infected with mycoplasma. Nature. 1965;207(992):43–5. [PubMed: 5866523]

19. Kagemann G, Henrich B, Kuhn M, Kleinert H, Schnorr O. Impact of Mycoplasma hyorhinis infection on L-arginine metabolism: differential regulation of the human and murine iNOS gene. Biol Chem. 2005;386(10):1055–63. [PubMed: 16218877]

20. Stanbridge E Mycoplasmas and cell cultures. Bacteriol Rev. 1971;35(2):206–27. [PubMed: 4935533]

21. Barile MF, Schimke RT, Riggs DB. Presence of the arginine dihydrolase pathway in mycoplasma. J Bacteriol. 1966;91(1): 189–92. [PubMed: 16562098]

22. Mitchell A, Finch LR. Pathways of nucleotide biosynthesis in Mycoplasma mycoides subsp. mycoides. J Bacteriol. 1977;130(3):1047–54. [PubMed: 324972]

23. Wang L, Westberg J, Bolske G, Eriksson S. Novel deoxynucleoside-phosphorylating enzymes in mycoplasmas: evidence for efficient utilization of deoxynucleosides. Mol Microbiol. 2001;42(4): 1065–73. [PubMed: 11737647]

24. Santos AP, Guimaraes AM, DoNascimento NC, Sanmiguel PJ, Martin SW, Messick JB. Genome of Mycoplasma haemofelis, unraveling its strategies for survival and persistence. Vet Res. 2011;42:102. [PubMed: 21936946]

25. Hatanaka M, Del Giudice R, Long C. Adenine formation from adenosine by mycoplasmas: adenosine phosphorylase activity. Proc Natl Acad Sci U S A. 1975;72(4):1401–5. [PubMed: 236559]

26. Mitchell A, Sin IL, Finch LR. Enzymes of purine metabolism in Mycoplasma mycoides subsp. mycoides. J Bacteriol. 1978;134(3): 706–12. [PubMed: 207675]

27. Zhang WC, Shyh-Chang N, Yang H, Rai A, Umashankar S, Ma S, et al. Glycine decarboxylase activity drives non-small cell lung cancer tumor-initiating cells and tumorigenesis. Cell. 2012;148(1–2):259–72. [PubMed: 22225612]

28. Patra KC, Hay N. The pentose phosphate pathway and cancer. Trends Biochem Sci. 2014;39(8): 347–54. [PubMed: 25037503]
29. Pithukpakorn M Disorders of pyruvate metabolism and the tricarboxylic acid cycle. Mol Genet Metab. 2005;85(4):243–6. [PubMed: 16156009]
30. Nunes-Nesi A, Araujo WL, Obata T, Fernie AR. Regulation of the mitochondrial tricarboxylic acid cycle. Curr Opin Plant Biol. 2013;16(3):335–43. [PubMed: 23462640]
31. Lillefosse HH, Clausen MR, Yde CC, Ditlev DB, Zhang XM, Du ZY, et al. Urinary loss of tricarboxylic acid cycle intermediates as revealed by metabolomics studies: an underlying mechanism to reduce lipid accretion by whey protein ingestion? J Proteome Res. 2014;13(5): 2560–70. [PubMed: 24702026]
32. Zabriskie TM, Jackson MD. Lysine biosynthesis and metabolism in fungi. Nat Prod Rep. 2000;17(1):85–97. [PubMed: 10714900]
33. Arruda P, Kemper EL, Papes F, Leite A. Regulation of lysine catabolism in higher plants. Trends Plant Sci. 2000;5(8):324–30. [PubMed: 10908876]
34. Tokovenko IP, Malynovs'ka LP. Features of amino acid assimilation by representatives of the Mycoplasma genus. Mikrobiolohichnyi zhurnal (Kiev, Ukraine: 1993). 2004;66(3): 58–63.
35. Hollenbeck CB. An introduction to the nutrition and metabolism of choline. Cent Nerv Syst Agents Med Chem. 2012;12(2):100–13. [PubMed: 22483274]
36. Ben-Menachem G, Mousa A, Brenner T, Pinto F, Zahringer U, Rottem S. Choline deficiency induced by Mycoplasma fermentans enhances apoptosis of rat astrocytes. FEMS Microbiol Lett. 2001;201(2):157–62. [PubMed: 11470355]

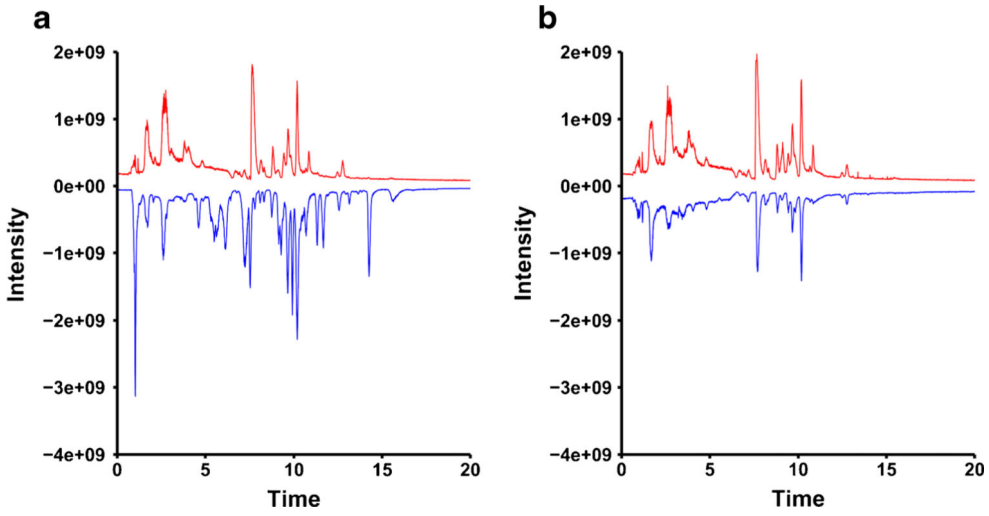

Fig. 1.

Mirror plot of representative total ion chromatograms (TIC) under positive (a) and negative (b) modes. TIC in *red*: mycoplasma-infected PANC-1 cells; TIC in *blue*: mycoplasma-free PANC-1 cells

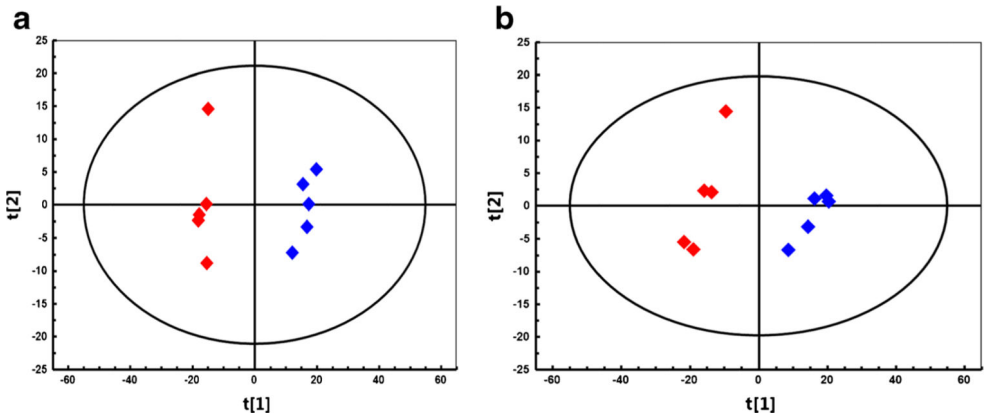

Fig. 2.

Principal component analysis under ESI positive mode (**a**) and ESI negative mode (**b**). *Red diamonds*: mycoplasma-infected PANC-1 cell samples; *blue diamonds*: mycoplasma-free PANC-1 cell samples

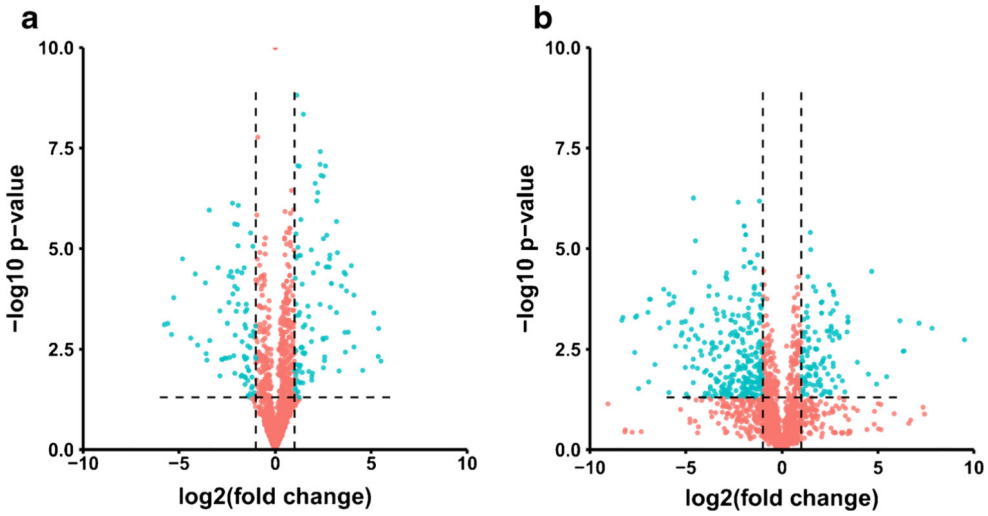

Fig.3.

Volcano plot based on fold change and *P* value of all metabolites in mycoplasma-infected and mycoplasma-removed PANC-1 cell samples under ESI positive mode (**a**) and ESI negative mode (**b**).Metabolite features of interest that display both large-magnitude fold change (fold change >2) as well as high statistical significance ($P<0.05$) are shown as *green dots*. Metabolite features that were abundant at similar levels (fold change <2) or were statistically nonsignificant ($P>0.05$) between the two groups are depicted as *red dots*

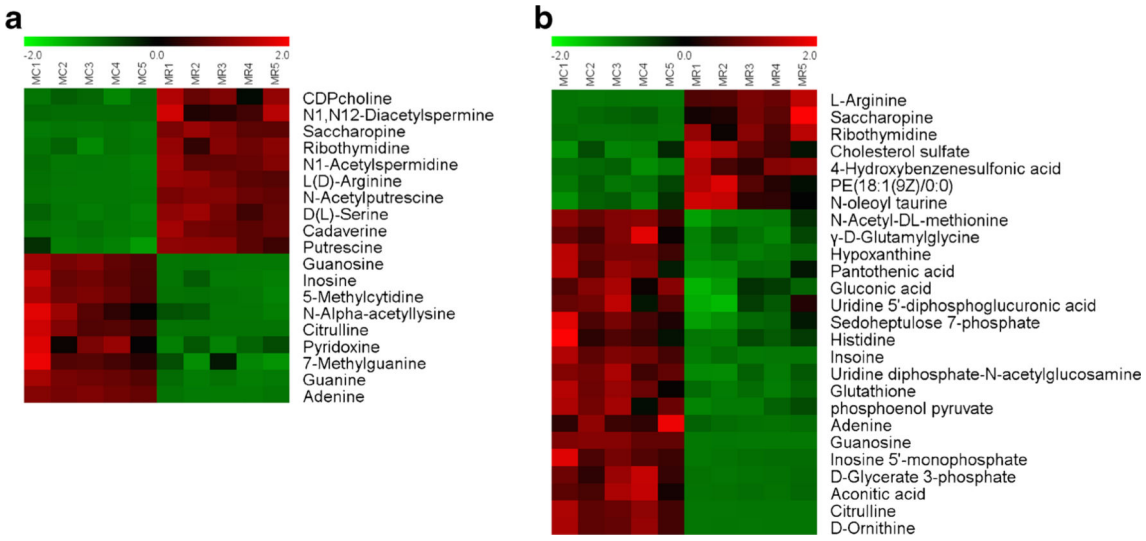

Fig. 4.

Heatmap of relative abundance of identified metabolites under ESI positive mode (**a**) and ESI negative mode (**b**). The *color* of each *square* is proportional to the significance of fold change of the metabolites. *Red*: increased levels; *green*: decreased levels. *MC*: mycoplasma-infected PANC-1 cell samples; *MR*: mycoplasma-free PANC-1 cell samples

Table 1

Identification of significantly changed endogenous metabolites in PANC-1 cells after mycoplasma infection

Metabolites	Trend[a]	Fold change	Retention time (min)	*m/z*	Mass error (ppm)	Related pathway
Positive mode						
L-Arginine	↓***	12.0	12.56	175.1192	1	Arginine metabolism
Saccharopine	↓***	9.0	13.84	277.1396	0	Biosynthesis of amino acids
D-Serine	↓***	4.0	8.99	106.0500	1	Biosynthesis of amino acids
CDP-choline	↓**	3.7	16.80	489.1152	1	Glycerophospholipid metabolism
Inosine	↑***	3.6	2.81	269.0881	0	Purine metabolism
Guanine	↑***	3.7	3.85	152.0568	0	Purine metabolism
Guanosine	↑***	12.3	3.69	284.0992	0	Purine metabolism
Adenine	↑***	37.0	3.52	136.0620	1	Purine metabolism
Citrulline	↑***	45.5	10.45	176.1032	1	Arginine metabolism
Negative mode						
L-Arginine	↓***	24.1	12.50	173.1045	0	Arginine metabolism
Saccharopine	↓**	6.3	13.95	275.1252	1	Biosynthesis of amino acids
Hypoxanthine	↑***	2.1	2.69	135.0313	0	Purine metabolism
Gluconic acid	↑***	2.2	8.33	195.0512	0	Pentose phosphate pathway
Sedoheptulose 7-phosphate	↑***	2.3	9.59	289.0334	1	Pentose phosphate pathway
Inosine	↑***	4.2	3.04	267.0737	0	Purine metabolism
Phosphoenol pyruvate	↑***	6.5	9.67	166.9752	0	TCA cycle glycolysis
Adenine	↑***	10.4	3.48	134.0474	1	Purine metabolism
Guanosine	↑***	10.4	4.10	282.0845	0	Purine metabolism
Inosine 5′-monophosphate (IMP)	↑***	12.5	9.63	347.0407	2	Purine metabolism
D-Glycerate 3-phosphate	↑***	14.7	14.25	184.9862	2	Biosynthesis of amino acids, glycolysis

Metabolites	Trend[a]	Fold change	Retention time (min)	*m/z*	Mass error (ppm)	Related pathway
Aconitic acid	↑***	15.2	2.54	173.0091	0	TCA cycle
Citrulline	↑***	58.8	10.43	174.0885	0	Arginine metabolism
D-Ornithine	↑***	66.7	10.43	131.0827	0	Arginine metabolism

The directionality of change after mycoplasma contamination is annotated as an increase or decrease in metabolite abundance

** $P<0.01$

*** $P<0.001$

[a] Change trend of the mycoplasma-removed group vs the mycoplasma-contaminated group